Immunology and Inflammation

Illuminating T cell-dendritic cell interactions in vivo by FlAsHing antigens

Reviewed Preprint

Published from the original preprint after peer review and assessment by eLife.

About eLife's process

Reviewed preprint posted
November 3, 2023 (this version)

Sent for peer review
September 6, 2023

Posted to Research Square
July 25, 2023

Munir Akkaya, Jafar Al Souz, Daniel Williams, Rahul Kamdar, Olena Kamenyeva, Juraj Kabat, Ethan M. Shevach, Billur Akkaya

The Ohio State University • National Institutes of Health • National Institute of Allergy and Infectious Diseases

Abstract

Delineating the complex network of interactions between antigen-specific T cells and antigen presenting cells (APCs) is crucial for effective precision therapies against cancer, chronic infections, and autoimmunity. However, the existing arsenal for examining antigen-specific T cell interactions is restricted to a select few antigen-T cell receptor pairs, with limited in situ utility. This lack of versatility is largely due to the disruptive effects of reagents on the immune synapse, which hinder real-time monitoring of antigen-specific interactions. To address this limitation, we have developed a novel and versatile immune monitoring strategy by adding a short cysteine-rich tag to antigenic peptides that emits fluorescence upon binding to thiol-reactive biarsenical hairpin compounds. Our findings demonstrate the specificity and durability of the novel antigen-targeting probes during dynamic immune monitoring in vitro and in vivo. This strategy opens new avenues for biological validation of T-cell receptors with newly identified epitopes by revealing the behavior of previously unrecognized antigen-receptor pairs, expanding our understanding of T cell responses.

eLife assessment

This study describes a method to track MHC class II binding peptides on dendritic cell (DC) surfaces using a tetracystein tag and a thiol-reactive dye, which can then be investigated in vitro and in vivo. This is a **valuable** study for the impact on immunology and potentially other areas where the detection of cell-associated peptides is required. The methods are **convincing** based on the use of MHC class I/II deficient mice that have significantly reduced signal, but the non-zero background is detected, and it is not clear that this is lower than if the peptides were directly labelled with fluorophores.

Introduction

The interactions between T cells and APCs form the cornerstone of adaptive immunity. Within the intricate milieu of lymphoid tissue, T cell priming stands out as a discrete and precise process, occurring amidst the multitude of dynamic cellular interactions. Multimerized peptide-major histocompatibility complex (pMHC) labeling has been the gold standard tool for capturing antigen-

specific T cells from a polyclonal repertoire [1]. However, such multimers, most commonly tetramers, have limitations in monitoring dynamic interactions of antigen-specific T cells in real-time due to their blocking effect on the immune synapse. Likewise, currently available T cell receptor like (TCRL), also known as peptide-in-groove (PIG), antibodies that detect pMHC complexes are known to disrupt the immune synapse, making them unsuitable for real-time monitoring of antigen-specific T cell interactions [2, 3]. Although alternative approaches for labeling antigenic peptides with conventional tags such as fluorescent proteins, fluorophores, and biotin-streptavidin have been used, these tags have limitations such as size constraints, membrane impermeability, and photophysically unstable nature, which restrict their use in applications for dynamic monitoring [4–7].

To overcome these drawbacks, we have developed a highly specific and minimally disruptive labeling strategy for studying antigen-specific T cell-APC interactions. Our approach involves introducing a six-amino acid tetracysteine tag (CCPGCC) on antigenic peptides and inducing fluorescence using membrane permeable thiol-reactive Arsenical Hairpin (AsH) probes [5, 8]. We have engineered the $OVA_{(323–339)}$ peptide by placing the tetracysteine tag at either the amino or the carboxy terminus, away from the TCR and MHC binding sites, to avoid disrupting T cell-APC synapse in vitro and in vivo [9].

Owing to these modifications, our labeling strategy preserves the T cell priming ability and allows for the detection of the fluorescent signal on the surface of APCs in a MHCII-dependent manner. Using flow cytometry and live microscopy, we found that the labeled peptide is readily taken up by the cognate $CD4^+$ T cells with precise specificity in vivo, as previously shown for pMHC complexes taken up from the immune synapse via processes such as trogocytosis and transendocytosis [10–14]. Furthermore, we have created new variants of the tetracysteine-tagged $OVA_{(323–339)}$ peptide with altered TCR-binding sites and have shown that the AsH probe labeling can track the TCR mediated uptake of nuanced pMHC complexes. This indicates that our labeling strategy is highly robust and forges a novel path for investigating immune responses against altered antigens such as those derived from self, microbiota and tumor microenvironment. Overall, AsH probe mediated immune monitoring offers significant advantages over existing methods, making it a versatile tool for in vitro and in vivo applications including live imaging of the T cell synapse within intact tissue architecture. This novel approach will further our understanding of T cell-mediated immune responses by also complementing tetramers for sorting antigen-specific T cells with precision and extending it to newly discovered epitopes.

Results

Signal intensity is determined by the sequence and placement of tetracysteine tag

We first generated $OVA_{323\ -\ 339}$ variants by placing a tetracysteine tag “CCPGCC” at amino or carboxy termini, either consecutively or via a flexible ε-amino-caproic acid (ε-ACA) linker to prevent endosomallysosomal enzymatic digestion to the tag. This yielded four variant peptides named as C- (carboxy terminus without linker), N- (amino terminus without linker), NACA- (amino terminus with ε-ACA) and CACA- (carboxy terminus with ε-ACA) (**Fig. 1a**). We used these variants to load mature C57BL/6 $CD11c^+$ splenic DCs from C57BL/6 mice and induced fluorescence by treating cells with Fluorescein-AsH (FlAsH) probe. Flow cytometry analysis showed that CACA-peptide combination but not the other tested variants induced a distinguished fluorescent signal (**Fig. 1b**). Cysteine is naturally oxidation prone and this may reduce FlAsH binding to tetracysteine tag. We addressed this problem by pre-treating OVA_{CACA} with tris-2-carboxyethylphosphine (TCEP), an irreversible reducing agent that blocks cystine disulfide bridge formation and elicited a consistent FlAsH signal (**Fig. 1c**). Moreover, we used another AsH probe excitable by 561 nm laser, called ReAsH, to occupy non-specific cysteine residues that would

otherwise attract FlAsH [15]. Pre-incubation of DCs with ReAsH improved signal to noise ratio significantly (**Fig. 1d**). We have created additional OVA variants to enhance signal intensity. These variants include one with two tetracysteine residues and another with a longer tetracysteine tag that withstands the British anti-Lewisite (BAL) wash, a crucial step to reduce background labeling by removing excess AsH probe [16]. However, new variants provided FlAsH intensity comparable to the original CACA variant, indicating no additional benefit for longer tags (**Fig. 1e**).

Tetracysteine tag does not alter the immunogenicity of peptide

Next, we sought to compare the $CD4^+$ T cell priming ability of four tetracysteine-tagged $OVA_{323-339}$ variants and that of native peptide in vitro. To do so, naïve $CD4^+$ T cells were isolated from $OVA_{323-339}$ specific TCR transgenic OTII mice, labelled with a proliferation dye and cocultured with mature $CD11c^+$ DCs that were pre-loaded with equimolar amount peptides for three days. Proliferation and activation status of OTII T cells were not altered by the presence or placement of the tag (**Fig. 2a-d**). Subsequently, DCs were pulsed with OVA_{CACA} vs. native peptide, treated with FlAsH and cocultured with fluorescently labeled OTII T cells for live confocal microscopy imaging. Within the first hours of coculture, OTII T cells established stable contact with OVA_{CACA}-pulsed DCs and FlAsH-labeled peptide gradually concentrated at the contact site (**Fig. 2e**). At 24 hours after treatment, OTII T cells in the peptide-treated groups exhibited increased volume and a shift towards a less spherical shape, indicative of T cell blasting (**Fig. 2f**). Furthermore, the interaction of T cells with OVA_{CACA} and native $OVA_{323-339}$ pulsed DCs resulted in a comparable decrease in T cell motility, suggesting that the tag had no impact on their dynamics in vitro (**Fig. 2g**).

Next, we performed a series of adoptive transfers to measure immunogenicity and signal persistence of tetracysteine-tagged peptides in vivo using two-photon microscopy and flow cytometry. Splenic DCs from β-Actin DsRed mice were pulsed with a peptide mix comprised of equimolar amounts of OVA-Biotin and OVA_{CACA}, where OVA-Biotin served as a positive control for flow cytometry. This was followed by ReAsH and optimized FlAsH treatments as indicated in **Fig. 1** and adoptive transfer into C57BL/6 recipients via footpad injection. Naïve $CD4^+$ T cells were isolated from OTII and WT C57BL/6 spleens, labelled with distinct cell-tracker dyes, mixed 1:1 and transferred into recipients via retroorbital i.v. injection (**Fig. 3a**). As previously demonstrated, adoptively transferred DCs were detectable in the popliteal lymph node 18–24 h post-transfer and they largely disappeared by 48 h [17–19]. FlAsH signal remained stable on DCs for the entire duration DCs were present in the lymph node (**Fig. 3b**). Strikingly, FlAsH was picked up by the cognate OTII T cells, suggestive of an antigen-specific peptide major histocompatibility complex II (pMHCII) trogocytosis in-vivo (**Fig. 3c, d**). Antigen-specific transfer was also confirmed by OVA-Biotin staining on OTII T cells by fluorochrome conjugated streptavidin (**Fig. 3c, d**). We had previously shown that antigen-specific Treg cells trogocytose pMHCII from DC synapse more efficiently than their effector CD4 + T cell counterparts [20]. To quantify FlAsH signal picked up by $OVA_{323-339}$-specific Treg cells, naïve OTII T cells were differentiated into induced Treg (iTreg) cells. While iTreg cells cocultured with antigen-pulsed DCs performed greater MHCII trogocytosis than naïve T cells at 18 h in vitro, peptide-specific trogocytosis was indiscernible within this time frame (Supplementary Fig. 1a-b). Similar to naïve OTII T cells, OTII iTreg cells acquired OVA_{CACA} and OVA-Biotin, with distinct peptide-specific signal and proliferative response on day 2 post-adoptive transfer (Supplementary Fig. 1c-f).

Intravital two-photon microscopy of the popliteal lymph node further confirmed the antigenicity of OVA_{CACA} in vivo by revealing the morphological changes compatible with T cell priming such as increased T cell volume and decreased sphericity (**Fig. 3e**). OTII-DC synapses had greater 3D volume and duration and harbored more FlAsH than surrounding regions (**Fig. 3g-h**). Overall, FlAsH signal was exclusively picked up by OTII T cells imaged, as early as 18 h (**Fig. 3i**, **Supplementary video 1**).

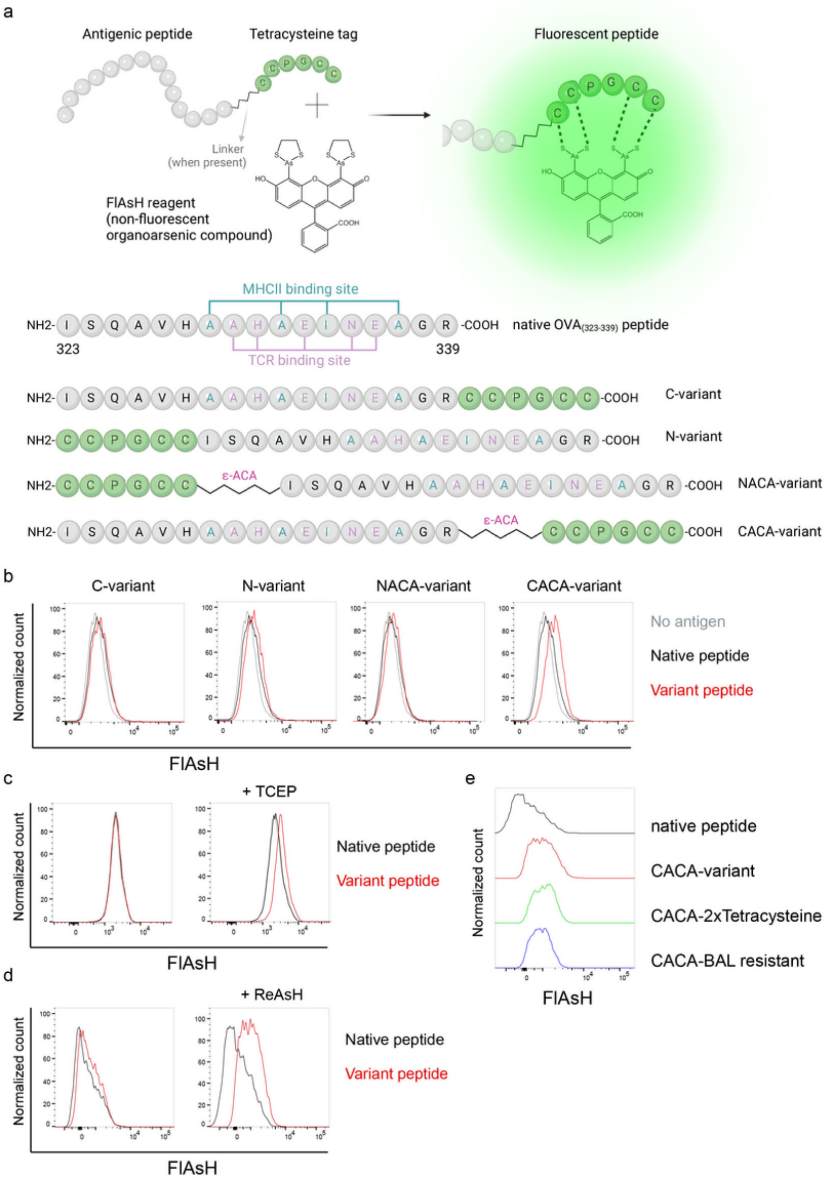

Figure 1

FlAsH labeling elicits fluorescence depending on the location of the tetracysteine tag.

a, AsH- probe labeling strategy for the tetracysteine-tagged peptides and the four $OVA_{323-339}$ variants generated for the study. **b**, FlAsH signal intensity on splenic DCs pulsed with tagged $OVA_{323-339}$ variants. **c**, FlAsH signal intensity on splenic DCs pulsed with CACA-variant following treatment with TCEP, a strong reducing agent. **d**, Signal intensity following pre-treatment of splenic DCs with ReAsH, followed by pulsing with CACA-variant and FlAsH treatment. **e**, FlAsH signal intensity of modified CACA-variant peptide with a duplicated CCPGCC sequence (CACA-2xTetracysteine) and CACA-variant peptide flanked with BAL-resistant peptide sequences (CACA-BAL resistant). Data in **b-d** are representative of three independent experiments, each performed with three biological replicates.

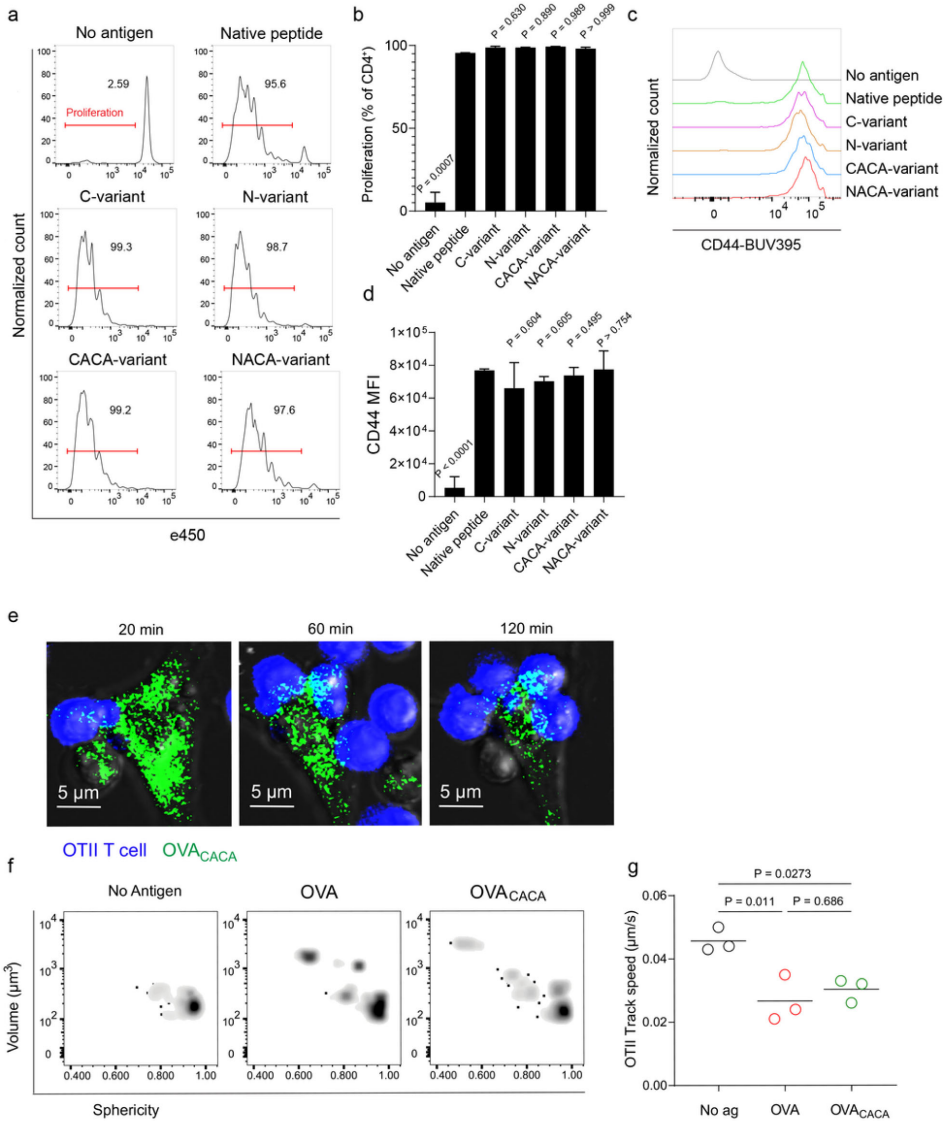

Figure 2

Tetracysteine tag does not alter the T cell priming ability of the native peptide.

a-d, DCs were loaded with the indicated peptides (5 µM) and co-cultured with e450-labeled naïve OT-II T cells (5×10^4) at a 1:10 DC to T cell ratio. **a**, Histograms (**a**) and the bar graph (**b**) demonstrate the proliferation status of T cells at 72 hours. Histograms (**c**) and the bar graph (d) depict the surface expression of CD44, a T cell activation marker. The bars (**b,d**) indicate the mean of three biological replicates; the error bars show the standard deviation. Data are representative of three independent experiments. P values refer to comparisons between each group and the native peptide, calculated using one-way ANOVA with Dunnett's multiple comparisons test. **e-g**, Peptide-pulsed DCs (2×10^5) were treated with FlAsH, cocultured 1:1 with e450-labeled naïve OT-II T cells and imaged for real-time interactions for 3 h (blue, OTII; green, FlAsH). **e**, Time lapse images depict the clustering of OTII T cells around OVA_{CACA}-pulsed DCs. **f**, Histocytometry plots for OTII T cell volume and sphericity. **g**, Graph shows the average track speed of OTII T cells. The lines mark the means of n = 3 replicates (one per symbol). Data are representative of two independent experiments. P values were calculated using a one-way ANOVA with Tukey's test.

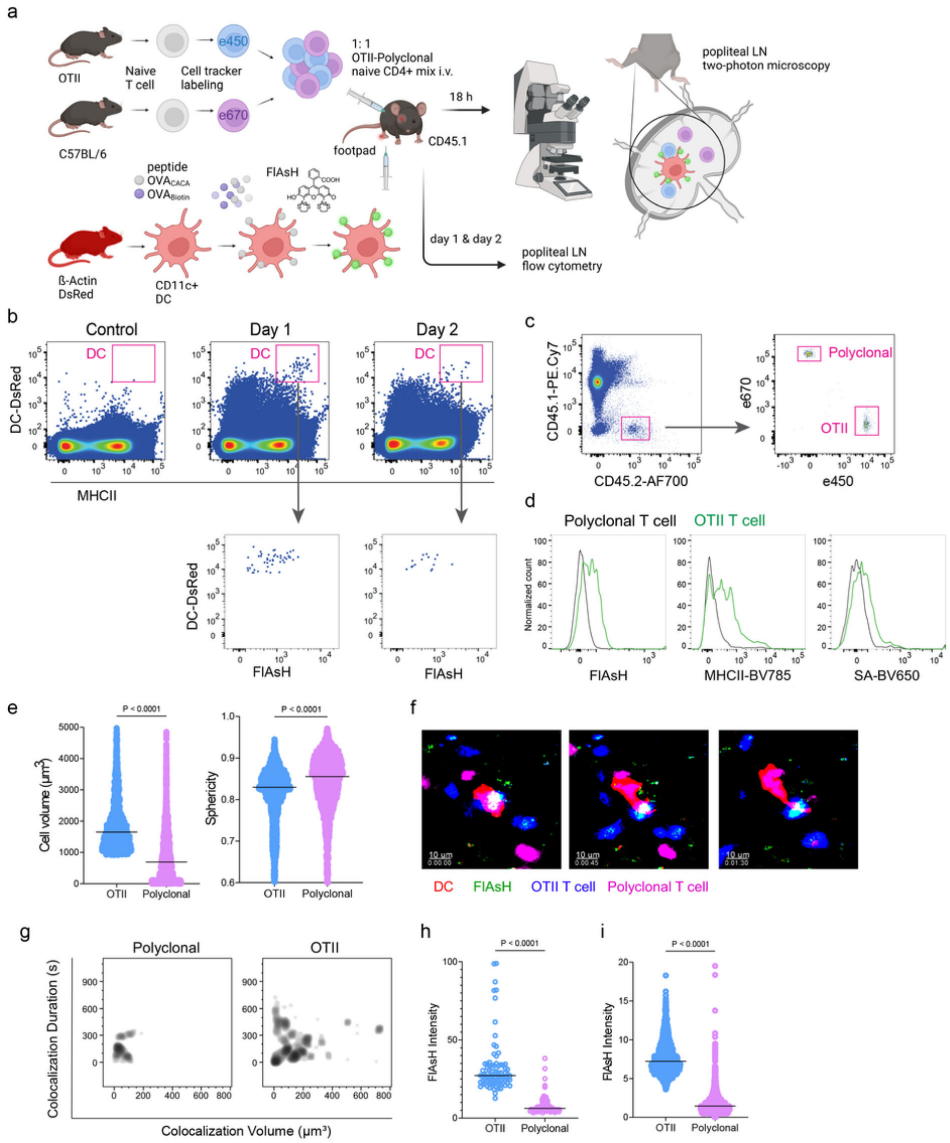

Figure 3

T cells acquire tetracysteine-tagged peptide from immune synapse.

DsRed^{+} splenic DCs were double-pulsed with 5 µM OVA_{CACA} and 5 µM OVA-biotin and adoptively transferred into CD45.1 recipients (2 × 10^6 cells) via footpad. Naïve e450-labeled OTII (1 × 10^6 cells) and e670-labeled polyclonal T cells (1 × 10^6 cells) were injected i.v. Popliteal lymph nodes were either imaged at 18 h or analyzed by flow cytometry at 18 h or 48 h post-transfer. **a**, Experimental approach. **b**, Flow cytometry plots gating on DsRed+ DCs over 48h (top panel) and demonstrating the OVA_{CACA} levels (FlAsH, bottom panel). **c**, Gating strategy for T cells of the recipient (CD45.1) and donor (CD45.2). **d**, T cell levels of OVA_{CACA} (FlAsH), MHCII, and OVA-biotin (detected with streptavidin) at 48 h following adoptive transfer. **a-d**, Data are representative of three independent experiments with n=3 mice per time point. **e-i**, Summary data from live microscopy showing OTII cell blasting (**e**), DC-T cell interaction with 45 min intervals (**f**), plots for the DC-T cell contact duration and volume, graphs for the FlAsH intensity limited to the DC-T cell contact regions (**g-h**) and average Flash intensity acquired by T cells (**i**). Data are representative of four independent experiments with n=2 mice per experiment. P values were calculated using two-sided Welch's t-test.

AsH-probe robustly tracks pMHCII complexes

To delineate whether FlAsH labeling reports free vs. MHCII-bound peptide in cells, we initially assessed how surface MHCII expression of cells correlates with the OVA_{CACA}-FlAsH signal. C57BL/6 splenocytes were incubated with OVA-Biotin or OVA_{CACA} and peptide distributions among the T cells, B cells and DCs were quantified by flow cytometry using streptavidin or FlAsH (**Fig. 4a**). Both streptavidin and FlAsH signals correlated significantly with MHCII expression, providing the strongest signal in DCs, where $CD4^+$ T cells served as a negative control due to lack of MHCII expression in mouse T cells [21] (**Fig. 4b**). It is worth mentioning that streptavidin detection of biotinylated peptide is a viable option for quantifying peptide loading on cells. However, size and membrane impermeable nature of streptavidin make it unsuitable for assays that include live monitoring of the T-DC interaction [22]. Next, we addressed whether FlAsH labeling of OVA_{CACA}-pulsed DCs is dependent on the MHC expression. $CD11c^+$ DCs were isolated from MHCII single knockout or MHCI and II double knockout (KO) mice, labeled with tracking dyes and mixed 1:1 with WT C57BL/6 DCs. Subsequently, they were incubated with OVA_{CACA} and treated with ReAsH and FlAsH as in **Fig. 1** (**Fig. 4e**). To make a fair comparison between WT and KO DCs and minimize autofluorescence, we performed adoptive transfers, aiming to facilitate in vivo elimination of apoptotic and possibly defective KO DCs [23, 24]. Flow cytometry analysis of the draining lymph node demonstrated that WT DCs, but not MHCII KO DCs, harbored FlAsH. Two-photon microscopy of the lymph node further confirmed these findings, indicating that FlAsH robustly marks OVA_{CACA}-MHCII complexes (**Fig. 4e-h**).

To address how FlAsH acquisition from synapse marks antigen-specific vs. bystander T cells, DCs were labeled with ReAsH and cell membrane dye PKH-26, pulsed with OVA_{CACA}, $E\alpha_{(52–68)}$ or left unpulsed. Next, they were treated with FlAsH and injected into the recipient mice via footpad. Subsequently, 1:1 mixture of labeled naïve OTII and Eα-specific T cells were adoptively transferred into via retroorbital sinus i.v. and the popliteal lymph nodes of the recipients were removed 18 h after the transfer (**Fig. 5a**). Flow cytometry analysis showed that OTII and Eα-specific T cells both acquired PKH-26 from double-pulsed DCs, indicating that they captured DC cell membrane from synapse (**Fig. 5b**). This process is termed as TCR-mediated trogocytosis and has previously been described as a feature of the DC-T cell synapse [11]. Although both T cell types trogocytosed double-pulsed DC cell membrane, FlAsH signal was picked up only by OTII T cells, suggesting that FlAsH tracks pMHCII mobility with a high precision (**Fig. 5c**).

Furthermore, we visualized dynamic $CD4^+$ T cell-DC contact and pMHCII mobility in vivo. DCs were labeled with ReAsH and cell membrane dye PKH-26, pulsed with OVA_{CACA} and/or LCMV $GP_{(61–80)}$ and treated with FlAsH. Recipient mice were injected with unpulsed, OVA_{CACA} single or OVA_{CACA}- $GP_{(61–80)}$ double pulsed DCs via footpad along with a 1:1 mixture of labeled naïve OTII and SMARTA T cells i.v. via retroorbital sinus. Popliteal lymph node microscopy confirmed that OTII and SMARTA T cells had stable contacts with double-pulsed DCs (**Fig. 5d**, **Supplementary video 2**). Similar to Eα-specific T cells, SMARTA also failed to pick up FlAsH signal despite showing signs of antigen-specific contact such as increased volume, reduced sphericity and decreased track speed (**Fig. 5e-f**).

Tetracysteine-tagging of peptides provides a sensitive tool to visualize interactions with altered TCR affinity

The lack of adaptable antigen-targeted probes presents a significant obstacle in the dynamic visualization of antigen-specific immunity. To address this gap, we sought to determine robustness of tetracysteine tagging in visualizing nuanced pMHCII variants. We created three variants by introducing alanine mutations at the TCR binding residues 331, 333, and 335 of OVA_{CACA} (**Fig. 6a**). The mutations at 331 and 333, depicted as variants 1 and 2 respectively, were previously reported to abolish the binding of OTII TCR to $OVA_{323-339}$ [9]. Although the residue 335 is flanked between the core OTII TCR binding residues 333 and 336, mutant 335 was shown to elicit normal proliferative response in vitro [9]. We addressed how pMHCII uptake by T cells is

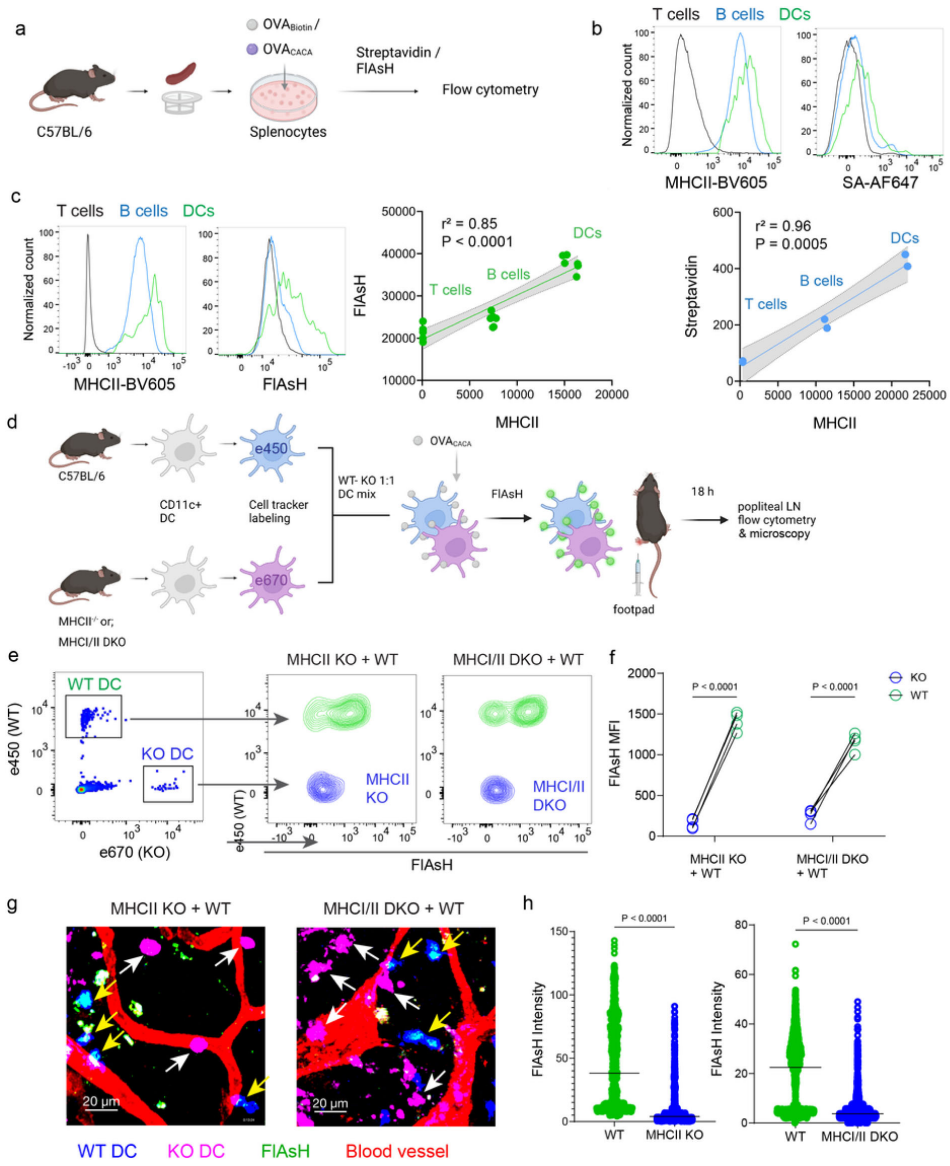

Figure 4

AsH probe reports the peptide loaded on the MHCII.

a-c, Relationship between surface MHCII expression and peptide load. **a**, Experimental scheme. **b**, Plots (top) show the surface levels of MHCII and OVA-biotin, graph (bottom) shows their correlation. Data are representative of two independent experiments performed with n = 2 biological replicates (one per symbol). **c**, Surface levels of MHCII and OVA_{CACA} (FlAsH) and their correlation. Data are representative of two independent experiments performed with n = 6 biological replicates (one per symbol). Simple linear regression and Pearson correlation and were used to demonstrate the relationship between surface MHCII and peptide load, gray area and dotted lines mark the standard error of the fitted line (**b**,**c**). **d**, Schematic depicting in vivo adoptive transfer approach. WT and KO DCs were labeled, mixed, pulsed with 5 µM OVA_{CACA}, labeled with FlAsH and adoptively transferred to WT recipients via footpad (1-2 × 10^6 cells). **e-f**, Flow cytometry plots (**e**) and graphs (**f**) showing FlAsH intensity of WT, MHCII-KO, or MHCI/II double-KO DCs that had migrated to the lymph node within 18 h following adoptive transfer. Data are representative of two independent experiments with n=4 mice per group. P values were calculated using two-sided Student's t-test. **g-h**, Microscopy images of popliteal lymph node following anti-CD31 (red) antibody injection i.v., yellow arrows point to WT, white arrows point to KO DCs (**g**), FlAsH intensity of adoptively transferred DCs (**h**). Data are representative of four independent experiments with n=2 mice per experiment. P values were calculated using two-sided Welch's t-test.

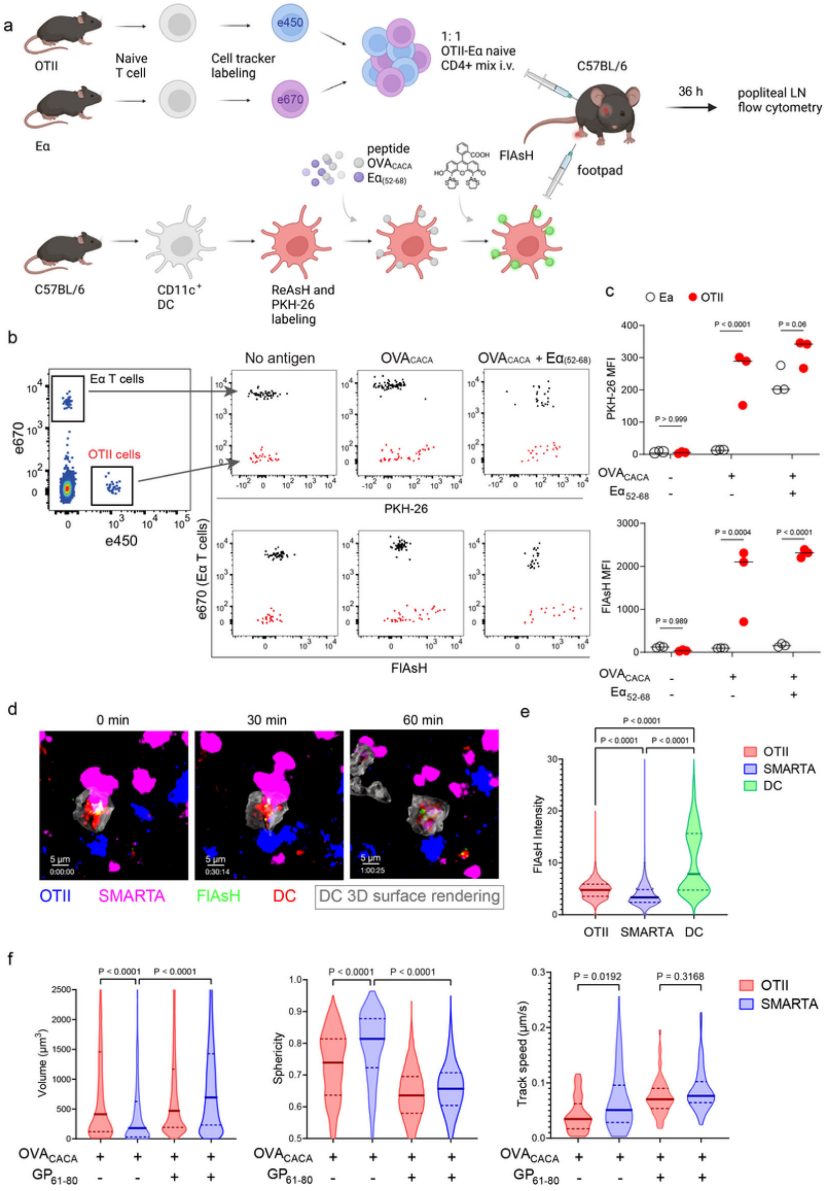

Figure 5

FlAsH-pMHCII is incorporated by cognate T cells in an antigen-specific manner.

a-c, DCs were labeled with ReAsH and PKH-26, single/ double-pulsed with 5 μM OVA_{CACA}, $Eα_{(52-68)}$ or left unpulsed. They were labeled with FlAsH and adoptively transferred into WT mice (0.5-1 × 10^6 cells) via footpad. Naïve e450-labeled OTII and e670-labeled Eα-specific T cells were mixed 1:1 (0.25-0.5 × 10^6/ T cell type) and injected i.v. Popliteal lymph node was analyzed by flow cytometry at 36 h post-transfer. **a**, Experimental scheme. **b**, Summary plots. **c**, PKH-26 and FlAsH MFI in OTII and Eα-specific T cells. Data are representative of two independent experiments with n=3 mice per group. P values were calculated using two-way ANOVA with Sidak's multiple comparisons test. **d-f**, DCs were labeled with ReAsH and PKH-26, single/ double-pulsed with 5 μM OVA_{CACA}, LCMV GP_{61-80}, labeled with FlAsH and adoptively transferred into WT mice (1-2 × 10^6 cells) via footpad. Naïve e450-labeled OTII and e670-labeled SMARTA T cells were mixed 1:1 (0.5-1 × 10^6/ T cell type) and injected i.v. Popliteal lymph node was imaged at 18 h. **d**, Time series representative of DC-T cell interactions. **e**, Average Flash intensity of the adoptively transferred cells. **f**, T cell blasting (left and middle panels) and motility (right) following adoptive transfer with DCs pulsed with the indicated peptides. Data are representative of three independent experiments with n=2 mice per group. P values were calculated using one-way ANOVA with Tukey's multiple comparisons test.

influenced by the mutation of TCR binding residues of OVA_{CACA}. DCs were isolated from CD45.1 congenic mice, loaded with variant peptides and cocultured with naïve CD45.2 OTII T cells for three days (**Fig. 6b-e**). In line with earlier observations, variants 1 and 2 interrupted T cell priming while variant 3 led to a proliferative response similar to native peptide (**Fig. 6c-d**). TCR mediated uptake of the FlAsH-labeled pMHCII complexes followed the same pattern and only variant 3 complexes produced a comparable signal to that of OVA_{CACA} (**Fig. 6e**). These suggest that AsH-probe labeling can be a sensitive method to track low affinity/ nuanced pMHCII complexes.

Discussion

Dynamic monitoring of antigen-specific T cell responses in vivo poses challenges due to the limited availability of reagents and the size constraints of the immune synapse. Here, we address this issue by presenting a novel strategy for visualizing T cell-APC interactions via tetracysteine tagging of antigenic peptides. While tetracysteine tagging has been previously applied in cell biology and virology, these applications have been mostly limited to cell lines and in vitro studies in immunology unrelated experimental settings [25–28]. On the other hand, our technique labels antigenic peptides and tracks pMHCII complexes in primary APCs during their interactions with T cells both in vitro and in vivo. Our approach is superior as compared to other strategies for monitoring T cell-DC interactions, in the way it robustly targets specific pMHCII complexes in real time in vivo. There is no need for special organisms or genetic modifications, and the technique can easily be expanded to new antigens and T cell-APC pairs from both mice and humans. This strategy can, for instance, be integrated into validation efforts for antigen discovery and utilized in the investigation of the synapses of newly deorphanized human T cells, a largely unexplored area where tools are scarce [29–32]. Given that is a two-part system (tag and FlAsH), it also carries the added capability of being inducible at different time points to allow for increased flexibility in interrogating pMHCII-TCR interactions over time. Our experiments demonstrate that tetracysteine-tagged peptides can be transferred from DCs to T cells via synaptic processes, such as antigen-specific pMHCII trogocytosis/transendocytosis, marking acceptor T cells for several days. Although the turnover of pMHCII in acceptor T cells requires further elucidation, our visualization of tetracysteine-tagged pMHCII can complement tetramers in detecting antigen-specific T cells in vivo. Additionally, we show that tetracysteine tagging of pMHCII does not broadly alter or disturb T cell-DC synapse. Therefore, our approach offers an advantage over tetramers in that it is suitable for real-time monitoring of the immune synapse. Finally, it is worth noting that tetracysteine tags can be visualized as electron-dense particles by Transmission Electron Microscopy [33, 34], providing potential for the detailed investigation of T-DC synapse and subcellular localization of pMHCII complexes. Although TEM application was out of scope for this study, it offers a promising avenue for future research. In conclusion, the tetracysteine labeling approach described here provides a powerful and unique tool to advance our understanding of T cell-APC interactions, offering new opportunities to investigate the immune response and develop improved immunotherapies.

Materials and Methods

Animals and reagents

C57BL/6, DsRed.T3, *H2-K1/H2-D1* knockout ($MHCI^{-/-}$), $E\alpha_{52-68}$, LCMV GP_{61-80}-specific (SMARTA) and $OVA_{323-339}$-specific (OT-II) TCR transgenic mice were acquired from The Jackson Laboratory. H2-Ab1 knockout ($MHCII^{-/-}$) mice were obtained from Taconic Biosciences. *H2-K1/D1*$^{-/-}$H2-Ab1$^{-/-}$

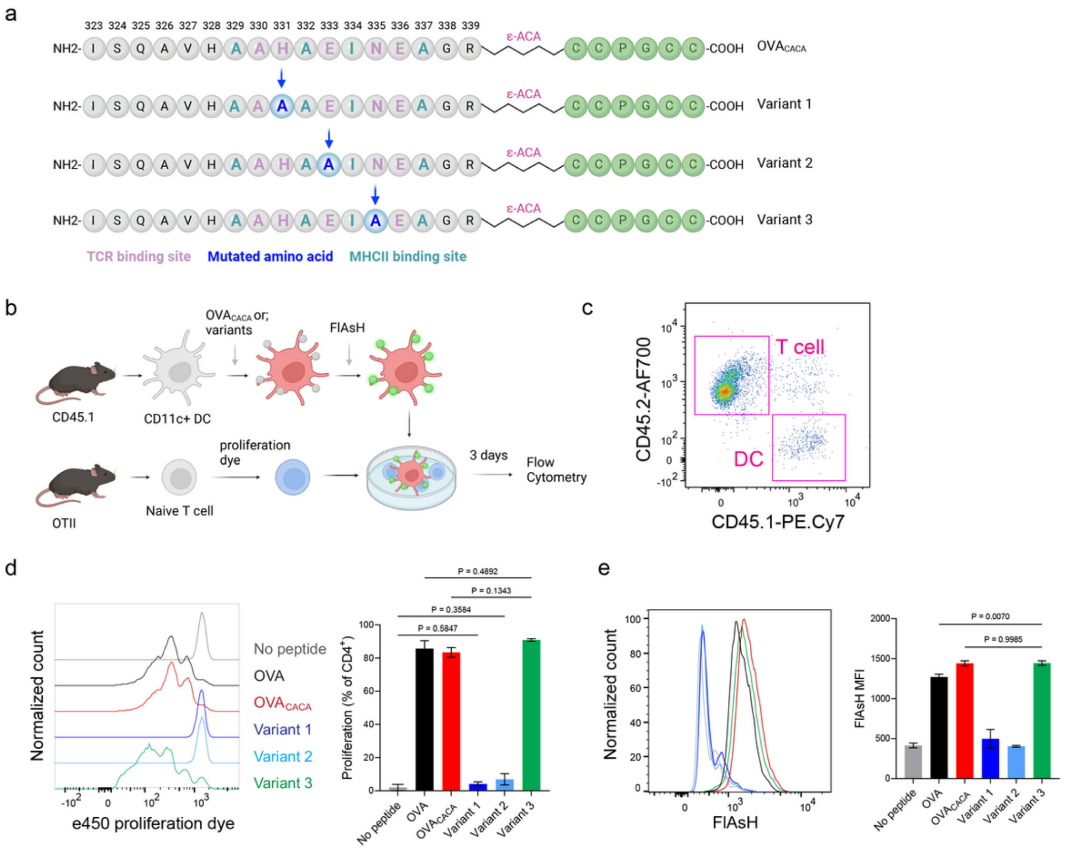

Figure 6

Nuanced TCR-pMHCII interactions can be discerned by FlAsH labeling of peptides.

a-b, Graphical depiction of the alanine-mutants for OVA_{CACA} TCR binding site and experimental approach. 0,5 × 10^5 $CD45.1^+$ DCs were pulsed with the indicated peptides, labeled with FlAsH and cocultured with 2,5 × 10^5 e450-labeled OTII cells for 3 days. **c**, Gating strategy for T cells and DCs. **d**, Representative flow cytometry plots for OTII T cell proliferation with a partial agonist (top) and two antagonist peptides (bottom). **e**, FlAsH signal intensity of DCs and OTII cells with partial agonist (top) and antagonist peptides (bottom) adoptive transfer with the indicated peptides followed by FlAsH treatment. Data are representative of two independent experiments performed with n = 3 biological replicates.

(MHCI-II double knockout) mice were obtained by breeding single knockout mice to homozygosity. All mice were maintained in Ohio State University ULAR and National Institutes of Health (NIH) animal facilities in compliance with Institutional Animal Care and Use Committee standards.

Cell cultures were maintained in sterile complete Roswell Park Memorial Institute (RPMI) media. The RPMI 1640 medium was supplemented with 10% heat-inactivated fetal bovine serum, 50 U/ml penicillin, 50 µM streptomycin, 1 mM sodium pyruvate, 2 mM L-glutamine, 0.1 mM non-essential amino acids, 50 µM 2-mercaptoethanol, and 10 mM HEPES (Thermo Fisher Scientific). For magnetic separations, cells were maintained in filtered and degassed magnetic-activated cell sorting (MACS) buffer. The MACS buffer consisted of PBS (Lonza) supplemented with 0.5% BSA (Sigma-Aldrich) and 2 mM EDTA (Sigma-Aldrich). For splenic dendritic cell (DC) isolation, Liberase TM (Blendzyme) and DNase I were purchased from Roche. 50 mg Liberase was dissolved in complete RPMI, resulting in a final concentration of 5 mg/mL. The solution was kept on ice, stirred gently every 5 minutes for 30 minutes and aliquoted into 1 mL portions. 10 mg/mL DNAse stock solution was prepared with 0.15 M NaCl and divided into 500 µL aliquots. Both enzymes were stored at -20ºC.

Samples were stained for flow cytometry using fluorescence-activated cell sorting (FACS) buffer (either PBS or Hanks' balanced salt solution (HBSS) supplemented with 2% fetal bovine serum, 1% HEPES, and 10 mM sodium azide (Sigma-Aldrich)). For confocal microscopy, PBS supplemented with 1% BSA was used. The antibodies used for flow cytometry are as follows: anti-CD4-efluor450 (clone GK1.5), anti-B220-PE (clone RA3-6B2), anti-CD11c-AF700 (clone N418), anti-CD45.1-PE.Cy7 (clone A20, Thermo Fisher Scientific), anti-CD45.2-AF700 (clone 104), anti-CD44-BUV395 (clone IM7, BD Biosciences), anti-I-A/I-E-BV605 (clone M5/114.15.2), anti-I-A/I-E-BV785 (clone M5/114.15.2), streptavidin-BV650, streptavidin-AF647 and purified anti-CD16/32 (clone 93). The antibodies were purchased from BioLegend unless stated otherwise. All peptides used in the study (**Supplementary Table 1**) were obtained from the NIH Research Technologies Branch, NIAID Peptide Core Facility.

For AsH probe labeling, peptides were pre-treated with fresh Tris Carboxy Ethyl Phosphene (TCEP, Sigma-Aldrich) to protect tetracysteine residues from oxidation. 10 mM ReAsH stock solution was prepared by adding 45 µL sterile cell-culture grade DMSO (Sigma-Aldrich) to 250 µg solid ReAsH (Cayman Chemical) and 10 mM FlAsH solution was prepared by adding 150uL DMSO to 1 mg FlAsH powder (Cayman Chemical). British Anti-Lewisite (BAL, Alfa Aesar) and HBSS with Ca^{++} and Mg^{++} (Thermo Fisher Scientific) was used to wash excess FlAsH off the cells. BAL is resuspended in sterile degassed water to obtain 8 mM stock solution. FlAsH, ReAsH and BAL are highly sensitive to oxidation, therefore their activity may decline in subsequent uses. This may be averted, at least in part, by quickly purging stock solution containers with 4M Argon gas (Sigma-Aldrich, 501247), placing container in a 50mL tube, purging again with Argon before storing FlAsH and ReAsH at -20ºC, BAL at 4ºC. We do not recommend storage longer than one month or repeated use of the same reagent stock.

DC isolation, peptide loading and -AsH probe labeling

Mature splenic DCs were isolated as previously described [35] and resuspended in complete RPMI. Peptides were added into 20 mM TCEP solution at twice the desired concentration for loading DCs. The solution was vortexed thoroughly and incubated at 37ºC for 30 minutes. Meanwhile, ReAsH stock solution was diluted to 100 uM in complete RPMI and added on DC suspension to obtain 1 uM final ReAsH concentration. Cells were incubated at 37ºC for 30 minutes and washed twice with complete RPMI. ReAsH labeled DCs were mixed with equal volume of peptide-TCEP solution, incubated at 37ºC for 30 minutes, washed twice and resuspended in complete RPMI to proceed with FlAsH labeling. Flash was added to cell suspension to achieve 1 uM final concentration, incubated at 37ºC for 30 minutes and washed twice with complete RPMI. To

remove excess FlAsH and reduce non-specific binding, cells were resuspended in 240 uM BAL diluted in HBSS with Ca^{++} and Mg^{++}, washed twice, then washed a third time with PBS and resuspended in PBS.

DC-T cell cocultures

Freshly isolated DCs were pulsed with peptide in complete RPMI and were incubated at 37°C for 30 min followed by three washes with complete RPMI to remove unbound peptide. Pulsed DCs were then treated with -AsH as decribed above then seeded into flat-bottom 96-well plates (Corning) at a density of 5 × 104 to 1 × 105 cells per well. T cells and iTreg cells were labeled with e450 or e670 (eBioscience) according to the manufacturer's protocol. Cells were cocultured at 37°C for for indicated periods, at a 1:10 ratio of DCs to T cells for proliferation assays and 1:1 for trogocytosis assays.

iTreg differentiation

For iTreg differentiation, Tnaive cells were isolated and 24-well sterile tissue culture plates (Corning) were coated with anti-CD3ε (BioLegend) and anti-CD28 (BioLegend) as described [36]. Naïve $CD4^+$ T cells were resuspended in complete RPMI media supplemented with 100 IU ml − 1 recombinant human IL-2 (Peprotech) and 5 ng ml − 1 recombinant human TGF-β (Peprotech). 3 × 10^5 cells were added to the wells at a volume of 1 ml per well. Cells were cultured at 37°C, 5% CO2 for 3–4 days.

Trogocytosis assay

Trogocytosis assays were perfomed as described in [20]. Briefly, freshly isolated splenic DCs were labeled with 4μM PKH26 (Sigma-Aldrich) for labeling of the cell membrane as described in Puaux et al.48. DCs were then pulsed with 10 μM peptide, treated with -AsH and were cocultured with T cells for up to 18 h. Cell conjugates were dissociated by washing cells with MACS buffer with 2 mM EDTA; cell suspensions were prepared for flow cytometry.

Flow cytometry

Cells were stained in FACS buffer containing fluorochrome-conjugated antibodies for 30 minutes at 4°C, protected from light. Data acquisition was performed with BD LSRFortessa and BD LSR II cytometers (BD Biosciences). Data analysis was performed with FlowJo v10.8.1.

Adoptive transfer

Mice were anesthetized in an induction chamber with 1.5% isoflurane USP (Baxter). Pulsed DCs were adoptively transferred through the right footpad in 50uL sterile PBS. T cells labelled with e450 or e670 (Thermo Fisher Scientific) were injected intravenously in 100uL sterile PBS through the retro-orbital sinus.

Confocal microscopy

35mm dishes with a 14mm glass coverslip bottom (MatTek) were pre-treated with 10ug/ml fibronectin (Sigma-Aldrich) in PBS for 1h at room temperature and washed twice. Splenic DCs were added onto the glass coverslip in complete RPMI and pulsed with 5–10 μM peptide at 37°C for 1 hour. Excess peptide was washed off with complete RPMI before addition of CD4 T cells. Co-cultures were imaged for 3-18h using a Leica SP-8 inverted microscope (Leica Microsystems) equipped with a full range of visible lasers, two hybrid detectors, three photomultiplier detectors, and a motorized stage. 63× objective (Leica Microsystems) was used and microscope configuration was set up for 3D analysis (x, y, z) of the cellular layer. The following lasers were used: diode laser for 405 nm excitation; argon laser for 488 and 514 nm excitation; diode-pumped solid-state laser for 561 nm; and HeNe laser for 594 and 633 nm excitation. All lasers were tuned to minimal power (between 0.3% and 2%) to prevent photobleaching. z stacking of images of 10–12 μm were

collected. Mosaic images of large cell culture areas (1 mm2) were generated by acquiring multiple z stacks using the Tile scan mode and were assembled into tiled images using LAS X v4.0 (Leica Microsystems).

Intravital two-photon laser-scanning microscopy of mouse popliteal lymph nodes

Mice were anesthetized in 1.5% isoflurane USP (Baxter) through a rodent nose cone followed by surgery to expose the right popliteal lymph node. Warm PBS was added to maintain lymph node moisture. Mouse body temperature was maintained with an infrared blanket (Braintree Scientific) throughout the imaging process after which they euthanized through cervical dislocation under anesthesia. Mice were imaged on a glass stage with a two-photon laser-scanning microscopy setup with a Leica SP8 inverted confocal microscope with dual multi-photon lasers, Mai Tai and InSight DS (Spectra-Physics), L 25.0 water-immersion objective, 0.95 NA (Leica Microsystems), and a 37°C incubation chamber (NIH, Division of Scientific Equipment and Instrumentation Services). The Mai Tai laser was tuned to 890 nm to excite e450and FlAsH; the InSight DS laser was tuned to 1,150 nm to excite DsRed/ PKH-26/ ReAsH and e670. For time-lapse imaging, a z stack consisting of 10–12 single planes (5 µm each over a total tissue depth of 50–60 µm) was acquired at 15 second intervals for a total period of 1–4 h.

Confocal microscopy of live lymph node sections

Live lymph node sections were imaged ex vivo using confocal microscopy. To maintain tissue architecture, popliteal lymph nodes were immediately transferred to PBS with 1% BSA and kept on ice immediately following harvest. Residual fat and connective tissue were removed using a Leica MZ6 StereoZoom microscope (Leica Microsystems). Lymph nodes were suspended in 38°C agarose in DMEM and kept over ice. Following complete agarose solidification, complete RPMI was added and blocks were cut containing one lymph node each. Lymph node blocks were cut into 200 µm sections with a Leica VT1000 S vibrating blade microtome (Leica Microsystems) at speed 5 in ice-cold PBS and frozen at -80°C. Prior to imaging, complete RPMI medium was added to tissue sections and incubated at 37°C for 2 h. Sections were held down with tissue anchors (Warner Instruments) in 35mm dishes with a 14mm glass coverslip bottom (MatTek) and were imaged with a Leica SP8 inverted five-channel confocal microscope equipped with an environmental chamber (NIH, Division of Scientific Equipment and Instrumentation Services) and a motorized stage. The microscope configuration was set up for four-dimensional analysis (x, y, z, t) of cell segregation and migration within tissue sections. A diode laser for 405 nm, an argon laser for 488 and 514 nm, a diode-pumped solid-state laser for 561 nm, and a HeNe laser for 594 and 633 nm excitation wavelengths were tuned to minimal power (between 0.3% and 2%). z-stack of images of 10–25 µm were collected. Mosaic images of whole lymph nodes were generated by acquiring multiple z stacks using a motorized stage to cover the whole lymph node area and assembled into a tiled image with the LAS X software. For time-lapse analysis of cell migration, tiled z stacks were collected over time (1–4 h).

Image analysis

Analysis of confocal and intravital two-photon images was performed using Imaris v9.2.1 and v10.0.0 (Bitplane) as previously described [35]. In brief, e450 and e670 signals were utilized for reconstructing the 3D structure of T cells and iTreg cells as surface objects. To reconstruct the 3D structure of DCs, overlapping DsRed, PKH-26, and ReAsH signals were employed. Imaris v10.0.0's built-in algorithms were used to calculate 3D volumes, track velocities, surface-to-surface colocalization parameters, and FlAsH (green) intensities of cells.

Statistical analysis

Statistical analysis was conducted on Prism v9.5.1 (GraphPad). Statistical tests and relevant P values for each figure are indicated in the figure or figure legend.

Acknowledgements

This study was funded by was by the National Institutes of Allergy and Infectious Diseases Intramural Research Grant ZIAAI000224, Extramural Research Grant DP2AI154451 and research funds from the Ohio State University College of Medicine.

Declarations

Author Contributions

B.A. conceived the project; B.A. and M.A. designed the experiments and wrote the manuscript; M.A., J.A.S., D.W., R.K., and O.K. performed the experiments; B.A. and J.K. analyzed the data; E.M.S., J.A.S. and, D.W. edited the manuscript.

Supplementary Files

3193191v1-video1.mp4 video/mp43193191v1-video2.mp4 video/mp4

reagent	MW	Sequence	Notes
OVA-4C-C	2340.65	ISQAVHAAHAEINEAGRCCPGCC	
OVA-4C-N	2340.65	CCPGCCISQAVHAAHAEINEAGR	
OVA-C-ACA	2453.81	ISQAVHAAHAEINEAGR-εACA-CCPGCC	
OVA-N-ACA	2453.81	CCPGCC-εACA-ISQAVHAAHAEINEAGR	
OVA-C-ACA x2	3020.53	ISQAVHAAHAEINEAGR-εACA-CCPGCCCCPGCC	x2
OVA-C-ACA (Re)	3185.95	ISQAVHAAHAEINEAGR-εACA-FLNCCPGCCMEP	BAL resistant
OVA-N-ACA (Re)	3185.95	FLNCCPGCCMEP-εACA-ISQAVHAAHAEINEAGR	BAL resistant
OVA-biotin	2000.4	ISQAVHAAHAEINEAGR-biotin	
OVA-C-ACA variant 1	2387.9	ISQAVHAAAAEINEAGR-εACA-CCPGCC	modified TCR binding site
OVA-C-ACA variant 2	2395.5	ISQAVHAAHAAINEAGR-εACA-CCPGCC	modified TCR binding site
OVA-C-ACA variant 3	2409.6	ISQAVHAAHAEIAEAGR-εACA-CCPGCC	modified TCR binding site

Supplementary table 1

The sequences and molecular weights of the peptides used in the study.

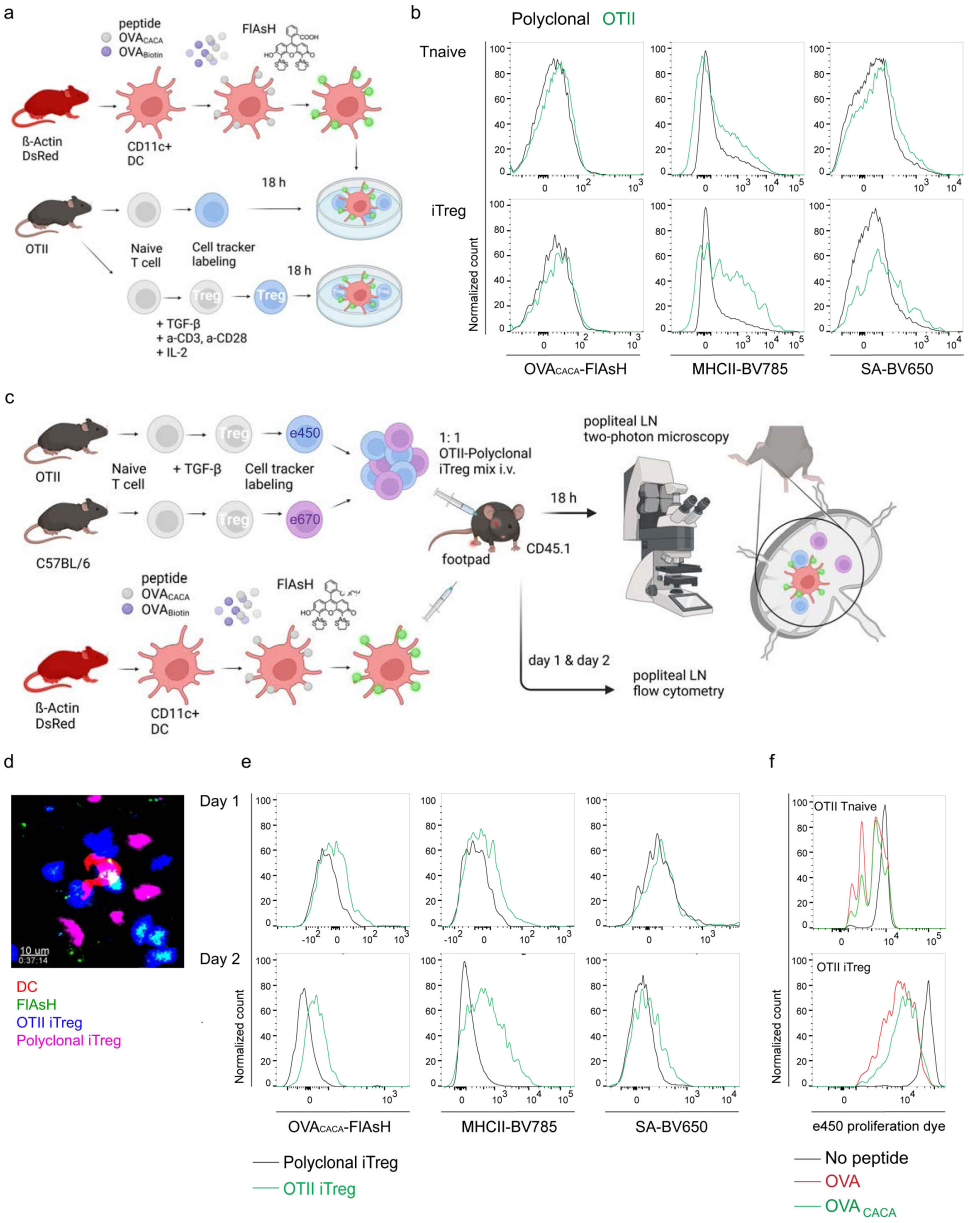

Supplementary Figure 1.

$OVA_{323-339}$-specific Treg cells acquire OVA_{CACA}-FlAsH from immune synapse

a-b, Naïve OTII and C57BL/6 (Polyclonal) T cells were differentiated into iTreg cells for 3-4 days. $DsRed^+$ DCs were double-pulsed with 5 µM OVA_{CACA} and OVA-biotin and cocultured 1:1 with e450-labeled naïve T cells or iTregs for 18 h. a, Experimental scheme. b, Overlaid histograms for the polyclonal and OTII T cell and iTreg levels of OVA_{CACA} (FlAsH), MHCII, and OVA-biotin (detected with streptavidin-BV650). Data are representative of two independent experiments performed with n = 3 biological replicates. c-f, Naïve OTII and C57BL/6 (Polyclonal) T cells were differentiated into iTreg cells, labeled with e450 and e670 respectively and injected i.v. into CD45.1 recipients (1-2 × 10^6 cells/ mouse per Treg type). 2-4 × 10^6 $DsRed^+$ DCs were double-pulsed with 5 µM OVA_{CACA} and 5 µM OVA-biotin and adoptively transferred via footpad. Popliteal lymph nodes were either imaged at 18 h or analyzed by flow cytometry at 18 h or 48 h post-transfer. c, Experimental approach. d, Summary data from live microscopy depicting DC-Treg cell interaction. e, Treg levels of OVA_{CACA} (FlAsH), MHCII, and OVA-biotin (detected with streptavidin-BV650) at 18 h (top) and 48 h (bottom) following adoptive transfer. f, Proliferation of OTII Tnaive and iTreg cells at 48 h following adoptive transfer with DCs that had been pulsed with indicated peptides. Imaging data are representative of two independent experiments with n=2 mice. Flow cytometry data are representative of three independent experiments with n=3 mice per group.

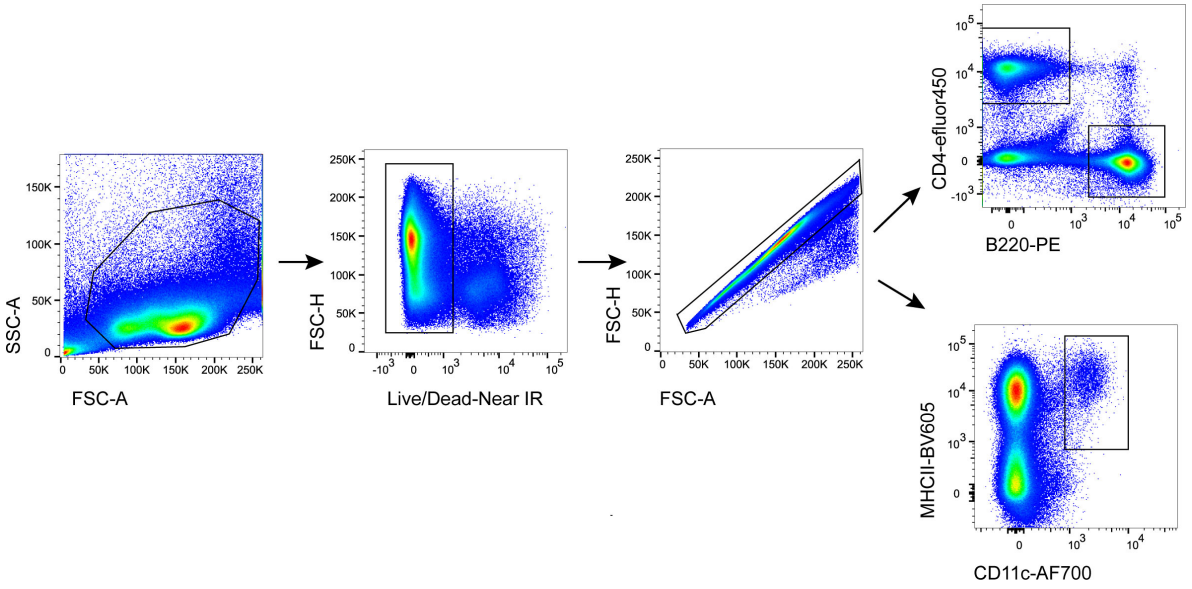

Supplementary Figure 2.

Sequential gating strategy for splenocytes to analyze CD4+ T cells, B cells and DCs.

References

1. Jenkins M.K. (2010) **On the composition of the preimmune repertoire of T cells specific for Peptide-major histocompatibility complex ligands** *Annu Rev Immunol* **28**:275–94

2. Dahan R., Reiter Y. (2012) **T-cell-receptor-like antibodies - generation, function and applications** *Expert Rev Mol Med* **14**

3. Hoydahl L.S. (2019) **Targeting the MHC Ligandome by Use of TCR-Like Antibodies** *Antibodies (Basel)* **8**

4. Giepmans B.N. (2006) **The fluorescent toolbox for assessing protein location and function** *Science* **312**:217–24

5. Hoffmann C. (2010) **Fluorescent labeling of tetracysteine-tagged proteins in intact cells** *Nat Protoc* **5**:1666–77

6. Toseland C.P. (2013) **Fluorescent labeling and modification of proteins** *J Chem Biol* **6**:85–95

7. Liu J., Cui Z. (2020) **Fluorescent Labeling of Proteins of Interest in Live Cells: Beyond Fluorescent Proteins** *Bioconjug Chem* **31**:1587–1595

8. Adams S.R. (2002) **New biarsenical ligands and tetracysteine motifs for protein labeling in vitro and in vivo: synthesis and biological applications** *J Am Chem Soc* **124**:6063–76

9. Robertson J.M., Jensen P.E., Evavold B.D. (2000) **DO11.10 and OT-II T cells recognize a C-terminal ovalbumin 323-339 epitope** *J Immunol* **164**:4706–12

10. Aucher A. (2008) **Capture of plasma membrane fragments from target cells by trogocytosis requires signaling in T cells but not in B cells** *Blood* **111**:5621–8

11. Daubeuf S. (2006) **A simple trogocytosis-based method to detect, quantify, characterize and purify antigen-specific live lymphocytes by flow cytometry, via their capture of membrane fragments from antigen-presenting cells** *Nat Protoc* **1**:2536–42

12. Wetzel S.A., McKeithan T.W., Parker D.C. (2005) **Peptide-specific intercellular transfer of MHC class II to CD4+ T cells directly from the immunological synapse upon cellular dissociation** *J Immunol* **174**:80–9

13. Hudrisier D. (2001) **Cutting edge: CTLs rapidly capture membrane fragments from target cells in a TCR signaling-dependent manner** *J Immunol* **166**:3645–9

14. Huang J.F. (1999) **TCR-Mediated internalization of peptide-MHC complexes acquired by T cells** *Science* **286**:952–4

15. Stroffekova K., Proenza C., Beam K.G. (2001) **The protein-labeling reagent FLASH-EDT2 binds not only to CCXXCC motifs but also non-specifically to endogenous cysteine-rich proteins** *Pflugers Arch* **442**:859–66

16. Machleidt T., Robers M., Hanson G.T. (2007) **Protein labeling with FlAsH and ReAsH** *Methods Mol Biol* **356**:209–20

17. Bajenoff M., Granjeaud S., Guerder S. (2003) **The strategy of T cell antigen-presenting cell encounter in antigen-draining lymph nodes revealed by imaging of initial T cell activation** *J Exp Med* **198**:715–24

18. Bousso P. (2008) **T-cell activation by dendritic cells in the lymph node: lessons from the movies** *Nat Rev Immunol* **8**:675–84

19. Ingulli E. (1997) **In vivo detection of dendritic cell antigen presentation to CD4(+) T cells** *J Exp Med* **185**:2133–41

20. Akkaya B. (2019) **Regulatory T cells mediate specific suppression by depleting peptide-MHC class II from dendritic cells** *Nat Immunol* **20**:218–231

21. Schooten E. (2005) **Lack of MHC-II expression in activated mouse T cells correlates with DNA methylation at the CIITA-PIII region** *Immunogenetics* **57**:795–9

22. Dundas C.M., Demonte D., Park S. (2013) **Streptavidin-biotin technology: improvements and innovations in chemical and biological applications** *Appl Microbiol Biotechnol* **97**:9343–53

23. Humblet-Baron S. (2019) **Murine myeloproliferative disorder as a consequence of impaired collaboration between dendritic cells and CD4 T cells** *Blood* **133**:319–330

24. Loschko J. (2016) **Absence of MHC class II on cDCs results in microbial-dependent intestinal inflammation** *J Exp Med* **213**:517–34

25. Griffin B.A., Adams S.R., Tsien R.Y. (1998) **Specific covalent labeling of recombinant protein molecules inside live cells** *Science* **281**:269–72

26. Mohl B.P., Roy P. (2017) **Elucidating virus entry using a tetracysteine-tagged virus** *Methods* **127**:23–29

27. Li S. (2022) **Tracking the Replication-Competent Zika Virus with Tetracysteine-Tagged Capsid Protein in Living Cells** *J Virol* **96**

28. Ng J.S.W. (2019) **Using Tetracysteine-Tagged TDP-43 with a Biarsenical Dye To Monitor Real-Time Trafficking in a Cell Model of Amyotrophic Lateral Sclerosis** *Biochemistry* **58**:4086–4095

29. Dobson C.S. (2022) **Antigen identification and high-throughput interaction mapping by reprogramming viral entry** *Nat Methods* **19**:449–460

30. Wang Y., Wang Z., Li G. (2022) **Engineered retroviruses map ligand-receptor interactions** *Nat Methods* **19**:408–410

31. Lewis S.A., Peters B. (2023) **T-cell epitope discovery and single-cell technologies to advance food allergy research** *J Allergy Clin Immunol* **151**:15–20

32. Pogorelyy M.V. (2022) **Resolving SARS-CoV-2 CD4(+) T cell specificity via reverse epitope discovery** *Cell Rep Med* **3**

33. Ellisman M.H. (2012) **Picking faces out of a crowd: genetic labels for identification of proteins in correlated light and electron microscopy imaging** *Methods Cell Biol* **111**:139–55

34. Cortese K., Diaspro A., Tacchetti C. (2009) **Advanced correlative light/electron microscopy: current methods and new developments using Tokuyasu cryosections** *J Histochem Cytochem* **57**:1103–12

35. Akkaya B. (2021) **Visualizing the Dynamics of T Cell-Dendritic Cell Interactions in Intact Lymph Nodes by Multiphoton Confocal Microscopy** *Methods Mol Biol* **2304**:243–263

36. Akkaya B. (2017) **Ex-vivo iTreg differentiation revisited: Convenient alternatives to existing strategies** *J Immunol Methods* **441**:67–71

Article and author information

Munir Akkaya
The Ohio State University

Jafar Al Souz
National Institutes of Health

Daniel Williams
National Institutes of Health

Rahul Kamdar
National Institutes of Health

Olena Kamenyeva
National Institutes of Health

Juraj Kabat
National Institutes of Health

Ethan M. Shevach
National Institute of Allergy and Infectious Diseases

Billur Akkaya
The Ohio State University
For correspondence: billur.akkaya@osumc.edu
ORCID iD: 0000-0002-6808-3776

Copyright

Editors

Reviewing Editor
Michael Dustin
University of Oxford, United Kingdom

Senior Editor
Satyajit Rath
Indian Institute of Science Education and Research (IISER), India

Reviewer #1 (Public Review):

Summary:
The authors develop a method to fluorescently tag peptides loaded onto dendritic cells using a two-step method with a tetracystein motif modified peptide and labelling step done on the surface of live DC using a dye with high affinity for the added motif. The results are convincing in demonstrating in vitro and in vivo T cell activation and efficient label transfer to specific T cells in vivo. The label transfer technique will be useful to identify T cells that have recognised a DC presenting a specific peptide antigen to allow the isolation of the T cell and cloning of its TCR subunits, for example. It may also be useful as a general assay for in vitro or in vivo T-DC communication that can allow the detection of genetic or chemical modulators.

Strengths:
The study includes both in vitro and in vivo analysis including flow cytometry and two-photon laser scanning microscopy. The results are convincing and the level of T cell labelling with the fluorescent pMHC is surprisingly robust and suggests that the approach is potentially revealing something about fundamental mechanisms beyond the state of the art.

Weaknesses:
The method is demonstrated only at high pMHC density and it is not clear if it can operate at at lower peptide doses where T cells normally operate. However, this doesn't limit the utility of the method for applications where the peptide of interest is known. It's not clear to me how it could be used to de-orphan known TCR and this should be explained if they want to claim this as an application. Previous methods based on biotin-streptavidin and phycoerythrin had single pMHC sensitivity, but there were limitations to the PE-based probe so the use of organic dyes could offer advantages.

Reviewer #2 (Public Review):

Summary:
The authors here develop a novel Ovalbumin model peptide that can be labeled with a site-specific FlAsH dye to track agonist peptides both in vitro and in vivo. The utility of this tool could allow better tracking of activated polyclonal T cells particularly in novel systems. The authors have provided solid evidence that peptides are functional, capable of activating OTII T cells, and that these peptides can undergo trogocytosis by cognate T cells only.

Strengths:
-An array of in vitro and in vivo studies are used to assess peptide functionality.
-Nice use of cutting-edge intravital imaging.
-Internal controls such as non-cogate T cells to improve the robustness of the results (such as Fig 5A-D).
-One of the strengths is the direct labeling of the peptide and the potential utility in other systems.

Weaknesses:
1. What is the background signal from FlAsH?
The baselines for Figure 1 flow plots are all quite different. Hard to follow. What does the background signal look like without FLASH (how much fluorescence shift is unlabeled cells to No antigen+FLASH?). How much of the FlAsH in cells is actually conjugated to the peptide? In Figure 2E, it doesn't look like it's very specific to pMHC complexes. Maybe you could double-stain with Ab for MHCII. Figure 4e suggests there is no background without MHCII but I'm not fully convinced. Potentially some MassSpec for FLASH-containing peptides.

2. On the flip side, how much of the variant peptides are getting conjugated in cells? I'd like to see some quantification (HPLC or MassSpec). If it's ~10% of peptides that get labeled, this could explain the low shifts in fluorescence and the similar T cell activation to native peptides if FlasH has any deleterious effects on TCR recognition. But if it's a high rate of labeling, then it adds confidence to this system.

3. Conceptually, what is the value of labeling peptides after loading with DCs? Why not preconjugate peptides with dye, before loading, so you have a cleaner, potentially higher fluorescence signal? If there is a potential utility, I do not see it being well exploited in this paper. There are some hints in the discussion of additional use cases, but it was not clear exactly how they would work. One mention was that the dye could be added in real-time in vivo to label complexes, but I believe this was not done here. Is that feasible to show?

4. Figure 5D-F the imaging data isn't fully convincing. For example, in 5F and 2G, the speeds for T cells with no Ag should be much higher (10-15micron/min or 0.16-0.25micron/sec). The fact that yours are much lower speeds suggests technical or biological issues, that might need to be acknowledged or use other readouts like the flow cytometry.